A New Dual Boost DC/DC Converter with a Voltage Conversion Gain

Jae-Jung Yun*

School of Electronic and Electrical Engineering, Daegu-University, Gyeongsan, S. Korea;
jjyun@daegu.ac.kr

Abstract

This paper presents the new boost dc/dc converter which has a high voltage conversion gain for the renewable energy source. To get a high voltage conversion gain, the proposed converter consists of the new two stage cascaded structure and has two voltage conversion processes. Due to the new structure and voltage conversion process, it has the higher output voltage conversion gain at the same duty ratio cycle than the conventional boost converter. To verify the performance and effectiveness of the proposed circuit was analyzed and tested by the PSIM simulator. The calculated power efficiency of the proposed circuit was 90.5% and the proposed circuit had the 3.5 times higher conversion ratio at the half duty cycle than the conventional dc/dc boost converter. Therefore, the superior voltage conversion ability of the proposed circuit is proved from the simulation results.

Keywords: Boost Converter, Cascaded Structure, High Voltage Gain

1. Introduction

In recent years, the boost dc/dc converters have been widely used to step-up the renewable energy sources in various industrial applications such as ESS, UPS, EV, etc. In those applications, a boost dc/dc converter generally steps up the low voltage sources (24-40 V) to the high voltage output (300-400 V). For that reasons, to obtain a high voltage gain, many converter topologies and methodologies were reported[1–18]. A step up power converter can be distinguished with the isolated and non-isolated structure. The dc/dc converter with the isolated structure using the high frequency transformer can provide high voltage gain and electric isolation, but it has large volume, many components, heavy weights, low cost effect and low power conversion efficiency. In case of the non-isolated structure which does not use a transformer, it can have smaller volume, fewer components, higher cost effectivity, higher power conversion efficiency than the isolated structure. Theoretically, the non-isolated type boost converter can achieve an infinite voltage conversion gain with the full

duty cycle. However, a practical boost converter has a limitation of a range of duty ratio due to turn on/off delay time of gate components, parasitic resistance of the inductors and capacitors. Due to aforementioned problems, the practical boost converter normally can step up an output voltage to about two times the input voltage. To overcome these disadvantages of the isolated structure, many topologies using coupled inductors, switched capacitors, and flyback based converters have been researched in the many previous papers[1–18].

The switched capacitor based converters in Figure 1 (a) can have the higher voltage conversion ratio than the traditional boost converter. However, to get the higher voltage conversion ratio, it has to use more switches, diodes and capacitors. Also, it makes difficult to control duty ratio of circuit[6–10].

A boost converter with a coupled inductor in Figure 1 (b) can adjust the voltage conversion ratio with the turn ratio of winding, but it makes a large input current ripple and the leakage inductance problem. To alleviate the voltage spike problem due to the leakage inductance,
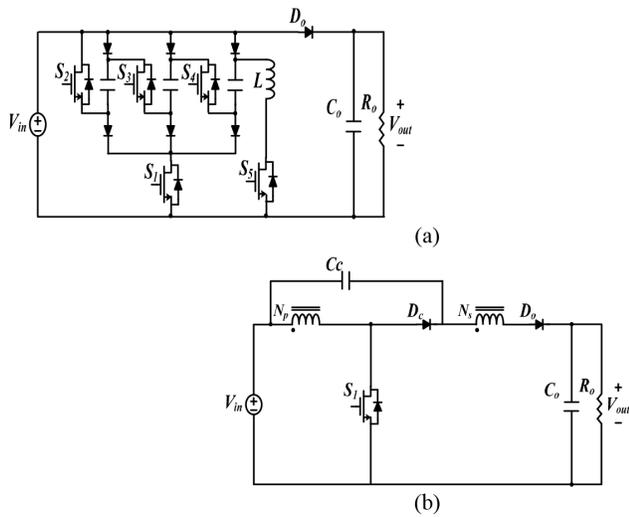
Figure 1. High voltage gain dc/dc converters; (a) Switched capacitor based converter in[1], (b) Coupled inductor based converter in[2]
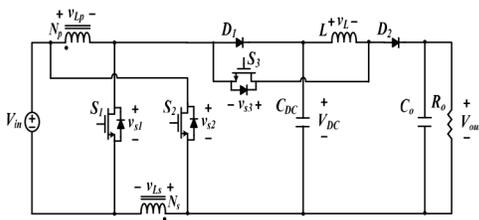

Figure 2. Configuration of the proposed step up converter.

the passive or active snubber circuits have been used. Unfortunately, it lowers the cost effectivity and increase the volume[11–13].

To solve the aforementioned problems, a new boost converter, which has the two stage cascaded structure and two voltage conversion processes, is proposed; it can achieve the high voltage gain. In addition, due to the DCM (Discontinuous Conduction Mode) operation of the coupled inductor, the proposed circuit does not have the voltage spike problem of the leakage inductance. The structure and operational principles are described in Section 2. The comparison of voltage conversion ratio with conventional circuit is given in Section 3.

The simulation results are reported in Section 4 and a conclusion is given in Section 5.

2. Proposed Ciruits and Operational Principle

The proposed boost converter (Figure 2) consists of three switches (S_1, S_2, S_3), two freewheeling diodes (D_1, D_2), a DC link capacitor (C_{DC}), an output voltage capacitor (C_o), a coupled inductor (N_p, N_s) and an inductor L. It achieves a high voltage conversion ratio thorough two power conversion stages. The proposed circuit has two the operation modes with the switching frequency $f_s = 1/T_S$ and a duty ratio of D. In the mode 1, the inductors (L, N_p, N_s) charge the magnetic energy and three switches (S_1, S_2, S_3) make the charging paths. In mode 2, the inductors (L, N_p, N_s) discharge the magnetic energy through the two freewheeling diodes (D_1, D_2). In operation modes, the theoretical waveforms and equivalent circuits are given in the Figures 3 and 4, respectively. To obtain those, the follows assumptions are made: 1) The winding turns of coupled inductor (N_p, N_s) are same, 2) The switches and diodes are ideal components, 3) All the capacitors and inductors are lossless, 4) The capacitors C_{DC}, C_o are sufficiently large and 5) The proposed circuit operates at Continuous Conduction Mode (CCM).

As a coupled inductor of the proposed boost converter has the same winding turns at the primary and secondary parts, the primary inductance L_p and secondary inductance L_S are same. Therefore, the following equations relating to the coupled inductor should be satisfied.

$$L_p = L_s = L \tag{1}$$

$$M = k\sqrt{L_1 L_2} = kL \tag{2}$$

$$v_{Lp} = L_p \frac{di_{Lp}}{dt} + M \frac{di_{Ls}}{dt} = L \frac{di_{Lp}}{dt} + kL \frac{di_{Ls}}{dt} \tag{3}$$

$$v_{Ls} = M \frac{di_{Lp}}{dt} + L_s \frac{di_{Ls}}{dt} = kL \frac{di_{Lp}}{dt} + L \frac{di_{Ls}}{dt} \tag{4}$$

Where k and M are the coupling coefficient and mutual inductance of the coupled inductor respectively. And, v_{Lp} and v_{Ls} are the voltages of the primary and secondary parts of the coupled inductor, respectively.

Mode 1 Figure 4(a), to<t<t1: At t0, S1, S2, S3 are turned on and D1, D2 are turned off. Consequently, the current of a coupled inductor increases. The voltage and current of the coupled inductor are as follows:
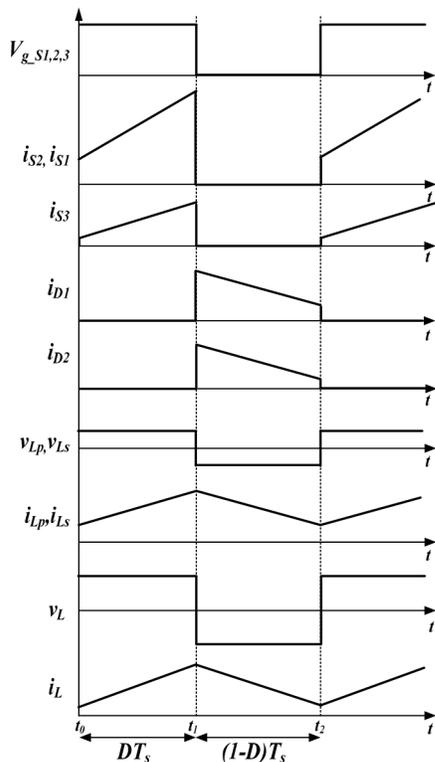
$$v_{Lp} = v_{Ls} = V_{in} \tag{5}$$

Figure 3. Theoretical waveforms of the proposed step up converter during a switching period.

$$i_{Lp} = i_{Ls} \tag{6}$$

$$\frac{di_{Lp}}{dt} = \frac{di_{Ls}}{dt} = \frac{V_{in}}{(1+k)L} \tag{7}$$

At the same time, to get high voltage conversion ratio, the current of inductor L simultaneously increases with the coupled inductor. The applied voltage to inductor L is (8).

$$v_L = V_{DC} + v_{Ls} \tag{8}$$

All of inductors store the magnetic energy in this mode.

Mode 2 Figure 4b, $t_1 < t < t_2$: At t_1, S_1, S_2, S_3 are turned off and D_1, D_2 are turned on. As a result, the current of a coupled inductor decreases. The voltage and current of the coupled inductor are as follows:

$$v_{Lp} + v_{Ls} = v_{in} - V_{DC} \tag{9}$$

$$i_{Lp} = i_{Ls} \tag{10}$$

$$\frac{di_{Lp}}{dt} = \frac{di_{Ls}}{dt} = \frac{V_{in} - V_{DC}}{2(1+k)L} \tag{11}$$

The current of inductor L simultaneously decreases with the coupled inductor and the voltage applied to the inductor is (12).

$$v_L = v_{DC} - V_{out} \tag{12}$$

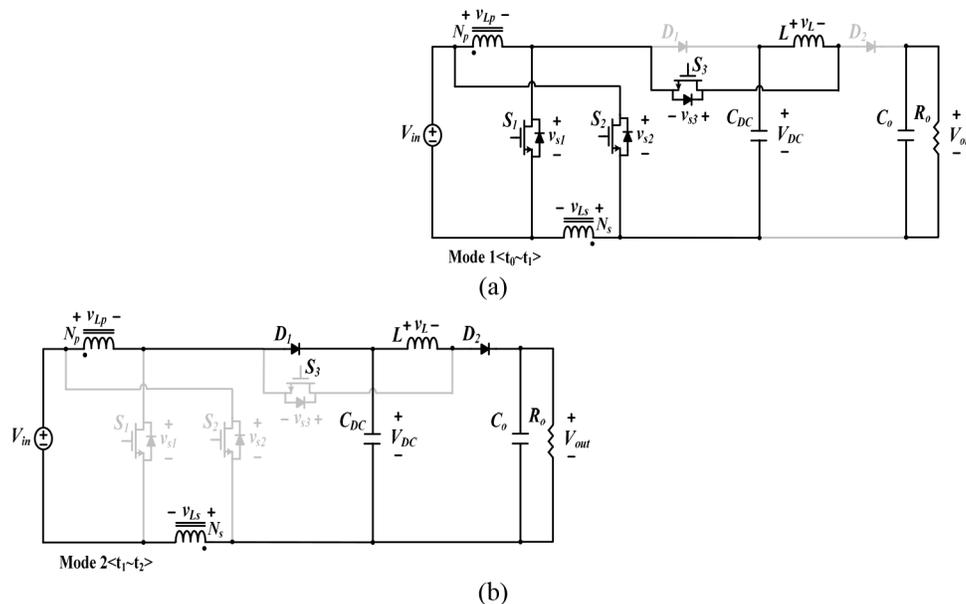In this mode, the magnetic energy starts to discharge to the load.

Mode 1 <t_0~t_1>

(a)

Mode 2 <t_1~t_2>

(b)

Figure 4. Theoretical waveforms of the proposed step up converter during a switching period.
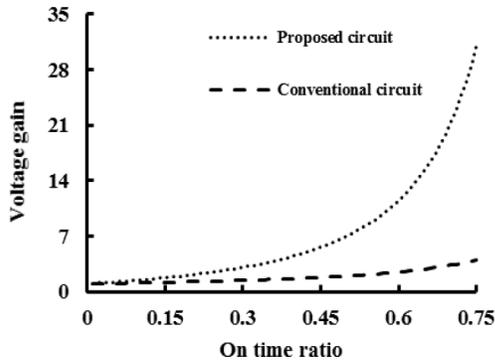
Figure 5. Output voltage gain of the proposed circuit.

Figure 6. Block diagram of the digital PI controller

3. Output Voltage Gain

The proposed boost converter has the two stage cascaded structure and two voltage conversion processes. At the first stage, the output voltage of the DC link capacitor (C_{DC}) is given by the voltage second balance principle of the energy of the coupled inductor. The output voltage of the DC link capacitor (C_{DC}) is derived from (7) and (11).

$$\frac{V_{in}}{(1+k)L}DT_s + \frac{V_{in} - V_{DC}}{2(1+k)L}(1-D)T_s = 0 \qquad (13)$$

Where V_{DC} is the output voltage of the DC link capacitor (C_{DC})

By simplifying (13), the following equation is obtained:

$$\frac{V_{DC}}{V_{in}} = \frac{1+D}{1-D} \qquad (14)$$

From (14), the output voltage of the DC link capacitor (C_{DC}) in the first stage is higher than that of the conventional DC-DC boost converter. At the second stage, the voltage second balance equation of the inductor L is given as:

$$(V_{DC} + v_{LS})DT_s + (v_{DC} - V_{out})(1-D)T_s = 0 \qquad (15)$$

Substituting equation (5) and (14) to (15), the final voltage conversion ratio of the proposed boost converter (Figure 5) is given as:

$$\frac{V_{out}}{V_{in}} = \frac{1 - D^2 + 2D}{\left(1-D\right)^2} \qquad (16)$$

Comparing with the voltage conversion ratio of the conventional boost converter given as (17), the proposed boost converter has the higher voltage conversion ratio:

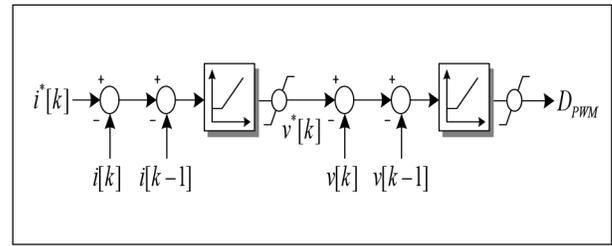$$\frac{V_{out}}{V_{in}} = \frac{1}{1-D} \qquad (17)$$

4. Simulation Result

To verify the high voltage gain ability of the proposed circuit, the circuit was simulated by using the PSIM simulator. The switching frequency of the boost converter is set as 100 kHz to ensure CCM at an inductor. The magnetizing inductance of the coupled inductor is selected as 400 uH and leakage inductance as 20 uH. An inductor is also selected as 2 mH for CCM operation. The capacitors have the different capacity (C_{DC} = 880 uF, C_o = 700 uF). The simulator was run at V_{in} = 50 V, V_{out} = 350 V and P_o = 300 W. In the simulation, the digital PI controller (Figure 6) was used to follow the output voltage and current reference value. To get the accurate and realistic results, the PSIM thermal modules were used for the simulation. They were the STW45N50 (MOSFET) from Microelectronics Company and ISL9R3060G2 (diode) from Fairchild Company.

The Figure7 shows the simulated waveforms of the main components. At the Figure 7, the switches (S_1, S_2, S_3) are turned on simultaneously during mode 1 and the switch currents (i_{sw_1}, i_{sw_2}, i_{sw_3}) are equal. At mode 2, the diodes D_1, D_2 transfer the magnetic energy of a coupled inductor and an inductor to the DC link capacitor and output capacitor. Finally, the DC link capacitor voltage is boosted to the output voltage. The simulation results show the simulated waveforms of the main components agree with the theoretical waveforms.
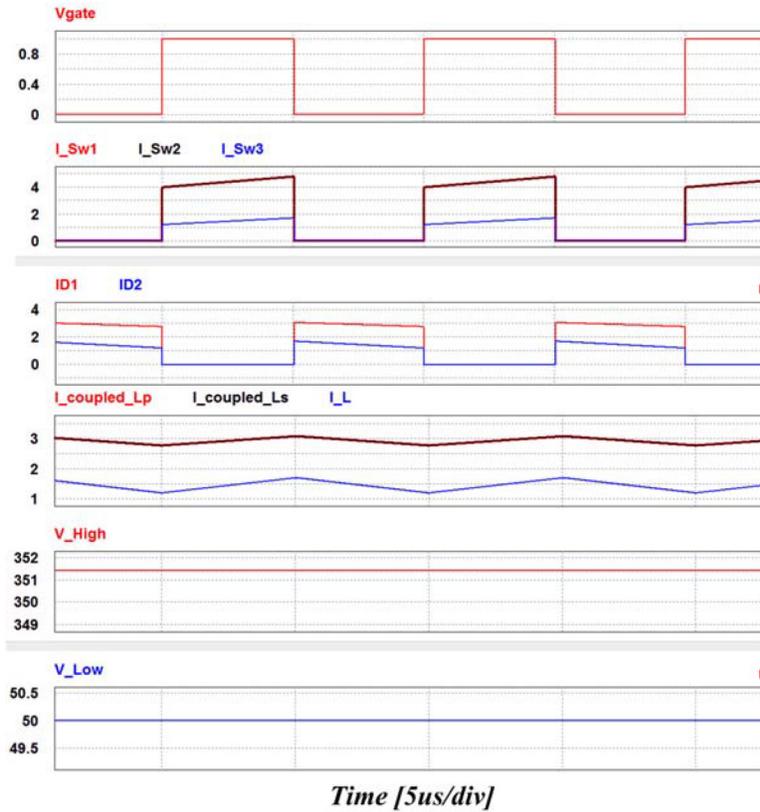
Figure 7. Current waveforms of switches, diode, inductors and gate signal at full load (300 W).
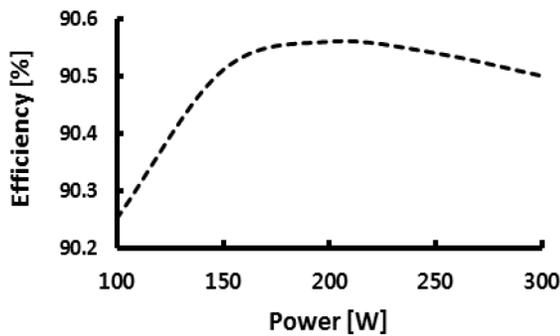

Figure 8. Power efficiency of the proposed converter versus output power

As shown in Figure 8, the power conversion efficiency of the proposed converter is 90.25%, 90.56% and 90.5% at the output powers of 100 W, 200 W and 300 W respectively.

5. Conclusion

A new dual boost dc/dc converter with the high voltage conversion ratio is proposed. The proposed boost converter is composed of three switches, two diodes, two capacitors, one coupled inductor and one inductor; it has the two stage cascaded structure and two voltage conversion processes. Due to the two voltage conversion processes with the coupled inductor of the first stage and the inductor of the second stage, the proposed has the higher output voltage gain than the conventional boost converter. The proposed circuit was simulated by the PSIM simulator. At the full load, efficiency of the proposed circuit was 90.5%. In addition, the proposed circuit brings the 3.5 times higher conversion ratio at the half duty cycle, when comparing with the conventional boost converter. The superior voltage conversion ability of the proposed circuit is proved from the theoretical analysis and simulation results.

6. Acknowledgment

7. References

1. Abutbul O, Gherlitz A, Bekovich Y, Ioinovici A. Step-Up switching-mode converter with high voltage gain using a switched capacitor circuit. IEEE Trans Ind Electron. 2003 Aug; 50(8):1098–102.

2. Zhang N, Suitanto D, Muttaqi KM, Zang B, Qiu D. High-voltge-gain quadratic boost converter with voltge multiplier. IET Power Electronics. 2015 Dec; 8(12):2511–9.

3. Yang LS, Liang TJ. Analysis and implementation of a novel bidirectional DC–DC converter. IEEE Trans Ind Electron. 2012 Jan; 59(1):422–34.

4. Freitas AAA, Tofoli FL, Sa Junior EM, Daher S, Antunes FLM. High-voltage gain DC-DC boost converter with coupled inductors for photovoltaic systems. IET power Electron. 2015 Oct; 8(10):1885–92.

5. Chen Z, Zhou Q, Xu J. Coupled-inductor boost integrated flyback converter with high voltage gain and ripple free input current. IET Power Electron. 2015 Feb; 8(2):213–20.

6. Chen YT, Tsai MH, Lian RH. DC-DC converter with high voltage gain and reduced switch stress. IET Power Electron. 2014 Oct; 7(10):2564–71.

7. Lee JY, Hwang SN. Nonisolated boost converter using voltage stacking cell. Electronic letters. 2008 May; 44(10):644–5.

8. Rosas-Caro JC, Mayo-Maldonado JC, Torres Espinosa HL, Valdex-Resendiz JE. A transformer-less high gain boost converter with input current ripple cancelation at a selectable duty cycle. IEEE Trans Ind Electron. 2013 Oct; 60(10):4492–9.

9. Barreto LHSC, Praca PP, Oliveira DS, Silva RNAL. High voltage gain boost converter basd on three commutation cell for battery charging using PV panels in a single conversion stage. IEEE Trans Power Electron. 2014 Jan; 29(1):150–8.

10. Silveira GC, Togoli FL, Bezerra LDS, Torrico-Bascople RP. A nonisolated DC-DC boost converter with high voltage gain and balanced output voltage. IEEE Trans Ind Electron. 2014 Dec; 61(12):6739–46.

11. Hu H, Gong C. A high gain input-parallel output-series DC-DC converter with dual coupled inductors. IEEE Trans Power Electron. 2015 Mar; 30(3):1306–17.

12. Chen SM, Lao ML, Hsieh YH, Liang TJ, Chen KH. A novel switched-coupled-inductor DC–DC step-up converter and its derivatives. IEEE Tran Ind Electron. 2015 Jan-Feb; 51(1):309–14.

13. Cecati C, Ciancetta F, Siano P. A multilevel inverter for photovoltaic systems with fuzzy logic control. IEEE Trans Ind Electron. 2010 Dec; 57(12):4115–25.

14. Yu X, Cecati C, Dillon T, Simoes MG. The new frontier of smart grid. IEEE Trans Ind Electron Mag. 2011 Sept; 15(3):49– 63.

15. Fontes G, Turpin C, Astier S, Meynard TA. Interactions between fuel cell and power converters: Influence of current harmonics on a fuel cell stack. IEEE Trans Power Electron. 2011 Mar; 22(2):670–8.

16. Amjadi Z, Williamson SS. Power-electronics-based solutions for plug-in hybrid electric vehicle energy storage and management systems. IEEE Trans Ind Electron. 2010 Feb; 57(2):608–16.

17. Henrique L, Barreto SC, Praca PP, Oliveira DS, Jr., Silva RNAL. High-voltage gain boost converter based on three-state commutation cell for battery charging using PV panels in a single conversion stage. IEEE Trans Power Electron. 2014 Jan; 29(1):150–8.

18. Hsieh YP, Chen JF, Liang TJ, Yang LS. Analysis and implementation of a novel single-switch high step-up DC–DC converter. IET Power Electron. 2012 Jan; 5(1):11–21.